p-ISSN 2089 – 0133 e-ISSN 2477-6416
URL : https://jurnal.uns.ac.id/ijap/article/view/89893
Indonesian Journal of Applied Physics (IJAP) Vol. 14 No. 2 page 353
DOI : https://doi.org/10.13057/ijap.v14i2.89893

EVALUATION OF FERRIC ION ADSORPTION ON THE SURFACE IMPRINTING ADSORBENT

Ihsan Alfikro[1,2], Jorena[1,3], Octavianus Cakra Satya[1], Erry Koriyanti[1], Fiber Monado[1], Idha Royani*[2,3]

[1]Departement of Physics, Faculty of Mathematics and Natural Sciences, University of Sriwijaya, Indralaya, Indonesia
[2]Master Program of Materials Science, Graduate School of Sriwijaya University, Palembang, Indonesia
[3]Laboratory of Material Science, Faculty of Mathematics and Natural Sciences, University of Sriwijaya, Indralaya, Indonesia
*idharoyani@unsri.ac.id

Received 07-07-2024, Revised 18-09-2024, Accepted 19-10-2024,
Available Online 19-10-2024, Published Regularly October 2024

ABSTRACT

Rapidity in technological aspects encourages industrial sector to utilize and apply the latest technology to accelerate and optimize production in its field. Thus, waste from industry polluting various aspects of environment, such as water, gives rise to environmental impacts. Heavy metals, including iron, are one of the most common and dangerous pollutants often found in water environments. The adsorption method has been used for separating heavy metals because of its simplicity, thus effectively cuts energy consumption and costs in process. However, the characteristics of heavy metal in water can vary depending on the element, which is essential to have deep understanding through it. This study, Fe(III)-IIPs was applied to adsorb and separate iron from water through repeated adsorption with parameter improvements. The pH parameter plays an important role, with ion competition happens at pH <2 and the formation of iron hydroxide species at pH >4.5, which results in adsorption inhibition. The system succeeds in separating 55% of iron content, with the average adsorption capacity at 8.4 mg/g within 30-minute equilibrium state. The modeling of the adsorption kinetic equation found that the adsorption system carries chemisorption characteristics (PSO), with maximum adsorption capacity of 11.15 mg/g and a reaction rate constant of 19 min^{-1}.

Keywords: Adsorption; Evaluation; Chemisorption; Fe(III); Imprinted polymer

Cite this as: Alfikro, I., Jorena., Satya, O. C., Koriyanti, E., Monado, M., & Royani, I. 2024. Evaluation of Ferric Ion Adsorption on The Surface Imprinting Adsorbent. *IJAP: Indonesian Journal of Applied Physics, 14*(2), 353-364. doi: https://doi.org/10.13057/ijap.v14i2.89893

INTRODUCTION

Adsorption is one of the most widely used technologies in wastewater treatment systems due to its advantages in terms of simplicity, ease, low cost, and low energy consumption [1]. High selectivity for sensor fabrication [2] and reusability for efficiency [3] are other advantages based on the characteristics of the adsorbent used. It can be dealt with on the principle of waste removal by the method of adsorption, which is based on the surface phenomenon, in which the adsorbent is attracted to the surface of the adsorbent due to some forces of attraction.

These forces can be electrostatic, due to differences in surface charge, or van der Waals force, which is an intermolecular dipole-dipole interaction, which in fact is a weak interaction known as physisorption. In addition, chemisorption interaction can also occur during the adsorption process, which involves electron transfer such as ion bonds or even covalents formed by chemical reactions, so the forces tend to be stronger. This is due to the presence of specific

binding sites formed on the surface of the adsorbent [4],[5]. Despite this, physisorption is reversible but non-selective process that allows the desorption to happen, while chemisorption is irreversible yet selective process [6].

Interactions during adsorption are reviewed on a molecular scale; therefore, external parameters such as pH, temperature, time, solvent volume, and adsorbent occupation greatly affect the performance of the adsorption system and its performance [7],[8],[9],[10],[11]. Moreover, the adsorption system needs to adjust to the target adsorbate since its characteristics can vary, such as reactivity and electric charge. Heavy metals are one of the highly reactive positive charge adsorbate that have been extensively studied for their toxicity and chemical characteristics. Hence, many adsorption systems have been developed to target specific heavy metals with different types of adsorbent [12]. Iron (Fe), as one of the heavy metals, has been found as a pollutant in many aspects of water, as it is the second most abundant metal that makes up the Earth's crust [13]. Iron is placed in group 8 on the periodic table as part of the metal transition along with ruthenium (Ru) and osmium (Os), based on the nomenclature system of IUPAC [14].

In water, iron can be present in two forms of cation: soluble Fe^{2+} and insoluble Fe^{3+}. In addition, some bacteria can oxidize iron into Fe^{3+} and stick to the plumbing system, damaging and polluting the waterways connected to each other, thus spreading very quickly [15]. Iron contamination in the human body is largely caused by long-term exposure to polluted drinking water, which accumulates in the body. Although iron plays an essential role in the metabolism of the human body, iron is potentially toxic to the body [16]. Iron poisoning, called hemochromatosis, can trigger complications of diseases such as cirrhosis and heart failure [17].

In this respect, it is important to be able to remediate iron residues from the water effectively and efficiently using simple adsorption methods. The study uses ion-imprinted polymers (IIPs) as adsorbents that have tested their selectivity properties against the target, thereby targeting only the target metal, Fe^{3+} ion [18],[19]. The adsorption system is based on a static system in which the Fe^{3+} adsorption is determined by Flame Atomic Absorption Spectroscopy (F-AAS) method. The study describes an assessment of the adsorption of Fe^{3+} on Fe(III)-IIPs, with differences in parameters such as pH and concentration during the adsorption process, accompanied by chemical characteristics of the Fe^{3+} ion in water.

METHOD

Materials

Polymers based on poly(methacrylic acid) (PMAA) are synthesized with the following ingredients: methacrylic acid (MAA/$C_4H_6O_2$) as functional monomer, ethylene glycoldimethacrylate (EGDMA/$C_{10}H_{14}O_4$) as crosslinker, benzoyl peroxide (BPO/$C_{14}H_{10}O_4$) 25% in H_2O used as initiator, $Fe(NO_3)_3 \cdot 9H_2O$ as iron template, hydrochloric acid (HCl) 37% in H_2O used as porogenic solvent, and gradient grade ethanol (C_2H_6O) as a solvent. Nitric acid (HNO_3) 65% in H_2O and the powder of sodium hydroxide (NaOH), respectively, were used to control acidity in the test solution. All materials are supplied by Merck & Co., Inc. and are used directly without further purification. The filter paper used in the filtration process is Whatman cellulose filter paper No. 41 (pores: 20 μm) and No. 42 (pores: 2.5 μm).

Synthesize of Fe(III)-IIPs

The pre-polymer solution was prepared by dissolving $Fe(NO_3)_3 \cdot 9H_2O$ into 40 mL of ethanol solution, then 0.4 mL of MAA, 3.96 mL of EDGMA, and 0.07 grams of BPO, respectively,

were added and homogenized at room temperature for 90 minutes. The polymerization was conducted by cooling-heating method, where the pre-polymer solution was subjected to a temperature of -5°C for 1 hour in order to remove the dissolved oxygen. Then the solution was heated at variations in temperature and heating time: 75°C for 3 hours, 80°C for 2 hours, and 85°C for 1 hour. The final result of polymerization was a solid acrylic-like polymer with transparent in color.

The solid polymer was grounded into a fine powder and washed several times using ethanol to remove impurities from the powder. The surface imprinting method was applied to remove the Fe3+ template from the polymer, thus creating cavities on its surface. The process was done by soaking the polymer powder in a solution of 6 M HCl, followed by stirring for 18 hours at 60°C. The process is repeated three times until the powder becomes pale yellow, called Fe(III)-IIPs, then neutralized to pH 7 with aquades. Finally, the powder was dried in the dessicator for 24 hours.

Stock Solution of Fe^{3+}

$Fe(NO_3)_3 \cdot 9H_2O$ was used to make 1000 ppm stock solution of Fe^{3+} in 100 mL of volumetric flask. A total of 0.723 g of $Fe(NO_3)_3.9H_2O$ was weighed and dissolved in a small amount of water. After being completely dissolved, the solution was transferred into the volumetric flask, and 30 mL of 1 M HNO_3 were added, then the water was added again until the solution touched the line of the volumetric flask at 100 ml. The same stock solution was made, but without the addition of HNO_3. The stock solution was diluted to obtain the test solution with the desired concentration.

Adsorption Experiment

Batch adsorption method, using Fe(III)-IIPs powder as adsorbent and Fe^{3+} ions as adsorbate. Adsorptions were carried out in a closed system, with the dosage of Fe(III)-IIPs and the initial concentration of Fe^{3+} ions determined. The filtrate was sent to the Shimadzu AA7000-series Flame-AAS spectrometer to measure the Fe^{3+} concentration remaining after adsorption. The adsorption experiment was performed in several stages and conditions, as follows:

Condition 1

Fe(III)-IIPs weighed 0.02 g were added to the Fe^{3+} solution at a concentration of 20 ppm, a volume of 20 mL, and a pH of 1.5; it was then left at room temperature with time variations of 10, 20, 30, 40, 50, and 60 minutes. The mixture was filtered using Whatman No. 42 filter paper.

Condition 2

Fe(III)-IIPs weighed 0.2 g were added to the Fe^{3+} solution at a concentration of 200 ppm, a volume of 20 mL, and 20 minutes of adsorption time; then left at room temperature with pH variations of 1; 1.5; 2.3; and 2.6. The mixture was filtered using Whatman No. 42 filter paper.

Condition 3

Fe(III)-IIPs weighed 0.02 g were added to the Fe^{3+} solution at a concentration of 20 ppm, a volume of 20 mL, 250 rpm stirring speed, and pH of 3.4. The solution was then left at room temperature with time variations of 10, 20, 30, and 40 minutes. The mixture was filtered using Whatman No. 42 filter paper.

Condition 4

Fe(III)-IIPs weighed 0.02 g were added to the Fe^{3+} solution at a concentration of 20 ppm, a volume of 20 mL, 250 rpm stirring speed, and at pH 4. Then the mixture was left at room temperature with time variations of 5, 15, 30, 45, and 60 minutes. The mixture was filtered using Whatman No. 41 filter paper.

RESULTS AND DISCUSSION

Characteristics of Iron Ion

The stock solution of Fe^{3+} was made with water as its solvent; consequently hydrolysis reaction occurs, which breaks down $Fe(NO_3)_3$ into ions based on the following reaction:

$$Fe(NO_3)_3 \rightleftarrows Fe^{3+} + 3NO^- \quad (1)$$

where this reaction release highly reactive Fe^{3+} ion, which binding hydroxyl group, thus forming a complex metal with water as its ligand molecule. The process consists of several stages [20]: (1) the formation of species with low molecular weight, as expressed in the following chemical reactions,

$$Fe^{3+} + 6H_2O \rightleftarrows Fe(OH_2)_6^{3+} + H_2O \rightleftarrows [Fe(OH_2)_5(OH)]^{2+} + H^+ \quad (2)$$

this reaction occurs spontaneously and slowly, (2) the formation of a red cationic polymer, (3) the degradation of a polymer that ends in conversion to the iron hydroxide phase, and (4) the deposition of the solid form of iron hydroxide, which begins at a solution with pH above 4.5 [21]. It's visibly characterized by a yellowish-brown color in the solution, as shown in Figure 1, and becomes more concentrated over time.

Figure 1. Stock solution of Fe^{3+} (left) and iron hydroxide begins to precipitate (right)

The hydrolysis of $Fe(NO_3)_3$ by water ligands should be prevented as soon as possible, as some Fe^{3+} ions will be separated from the solution and reduce the concentration of iron in the solution, especially when measured by analytical methods such as AAS. To prevent this, a concentrated HNO_3 can be added to shift the equilibrium of the reaction toward the side of the reagent, which is $Fe(NO_3)_3$. This is in line with the Le Châtelier principle, in which the balance will shift in the direction of the added substance (NO^{3-}) [22]. Hence, the reaction becomes,

$$[Fe(OH_2)_5(OH)]^{2+} + H^+ \xrightarrow{[HNO_3]} Fe(NO_3)_3.9H_2O \quad (3)$$

The change in color of this solution can be explained by the properties of iron as one of the transition metals since its electron configuration fills only part of the d-orbital, which is shown below,

$$_{26}\mathbf{Fe^0}=[\mathbf{Ar}]\ 3d^6\ 4s^2;\ \mathbf{Fe^{2+}}=[\mathbf{Ar}]\ 3d^6;\ \mathbf{Fe^{3+}}=[\mathbf{Ar}]\ 3d^5$$

therefore, iron(0) has electron valence of 8, which fills two different shells on its atom. While oxidized iron (Fe^{2+} and Fe^{3+}), will lose electrons on the subshell of 4s [22]. Figure 2 shows the solubility of $Fe(NO_3)_3$ at different pH, which shows $Fe(NO_3)_3$ starting to hydrolyze into iron hydroxide species at pH 3, which is shown with a change of color towards yellowish and starting to form precipitation along with rise in pH, as the process tends to be slow. At the basic pH, precipitation is rapidly formed because high concentrations of OH^- bind more iron ions.

This is the characteristic that gives metal solutions a particular color transition, including iron, which has a yellowish-brown color. This is due to the absorption of energy at certain wavelength in the visible spectrum of light by the complexation between iron and water as ligands. Water, H_2O, as a ligand, will react with iron due to the high reactivity of iron ions, but this process will create valence electrons on d-orbital—which is capable of holding 5 pairs of electrons—of the iron, which will be split, thus creating a difference in energy levels of the same orbital. d-orbital splitting is caused by Coulomb repulsion between the electron on the ligand and the electron in the d-orbital of iron. The Coulomb repulsion will be much higher at electrons closer to the ligand, causing the splitting of d-orbital. The complexation of water with iron makes the electron on the d-orbital able to excite to higher energy level by absorbing corresponding energy from the environment. It is known as the d-d transition [23].

Based on the UV-Vis spectra of $Fe(NO_3)_3$ solution in water observed by Sutherland et al. [24], there is an absorption peak at a wavelength of 380 nm, which refers to the purple color on the visible light spectrum. The author stated that nitrate ions, NO^{3-} do not absorb light above 300 nm, but species of iron hydroxide complex absorb light around wavelengths of 300 nm. This absorption is d-d transition on the complexation of iron ions and water, where the remaining visible light is transmitted, producing a complementary color of purple, i.e., yellow.

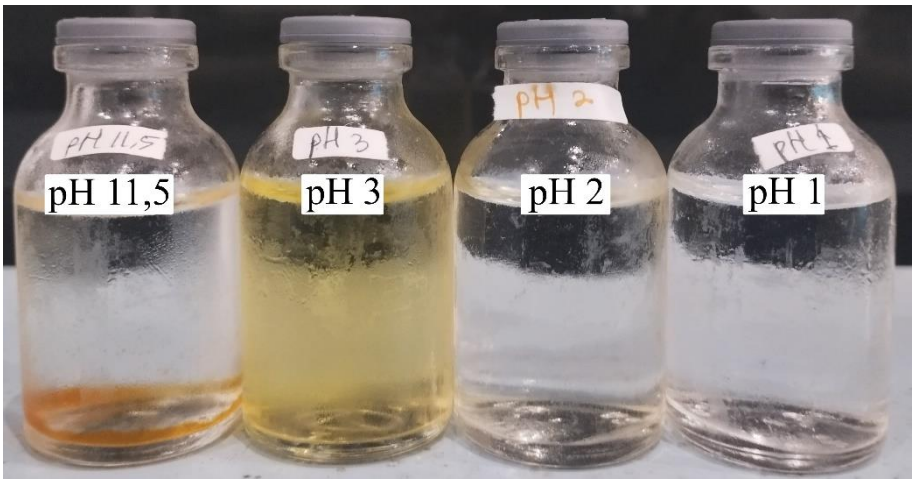

Figure 2. Solubility of $Fe(NO_3)_3$ on different pH

Evaluation of Adsorption System

The optimization of adsorption parameters becomes essential in order to enhance the adsorption of adsorbate on the adsorbent and diminish possible errors. This study displays several adsorption systems that have been performed and their evaluations based on similar

references. Figure 3 shows four different adsorption systems against Fe^{3+} ions on the same material, namely Fe(III)-IIPs.

In condition 1, the adsorption was performed with the time variation of 10–60 minutes. In this case, the Fe^{3+} solubility is high, but this is inconsistent with the adsorption results on the surface of Fe(III)-IIPs, with the average adsorption capacity and removal efficiency, respectively, only at 3.6 mg/g and 18%. Low adsorption performance in this system is due to the high acidity of the solution, i.e., at pH 1.5, which allows protonation of the active site of Fe(III)-IIPs, plus a competition exists between H^+ ions and Fe^{3+} ions during adsorption [25],[26]. Several articles reported similar things concerning the adsorption of metal ions at low pH [27],[28],[29],[30],[31],[32]. A drastic decrease in adsorption at minute 60 can be attributed to the desorption of Fe^{3+} ions from the surface of Fe(III)-IIPs due to the effects of acidity [33],[34].

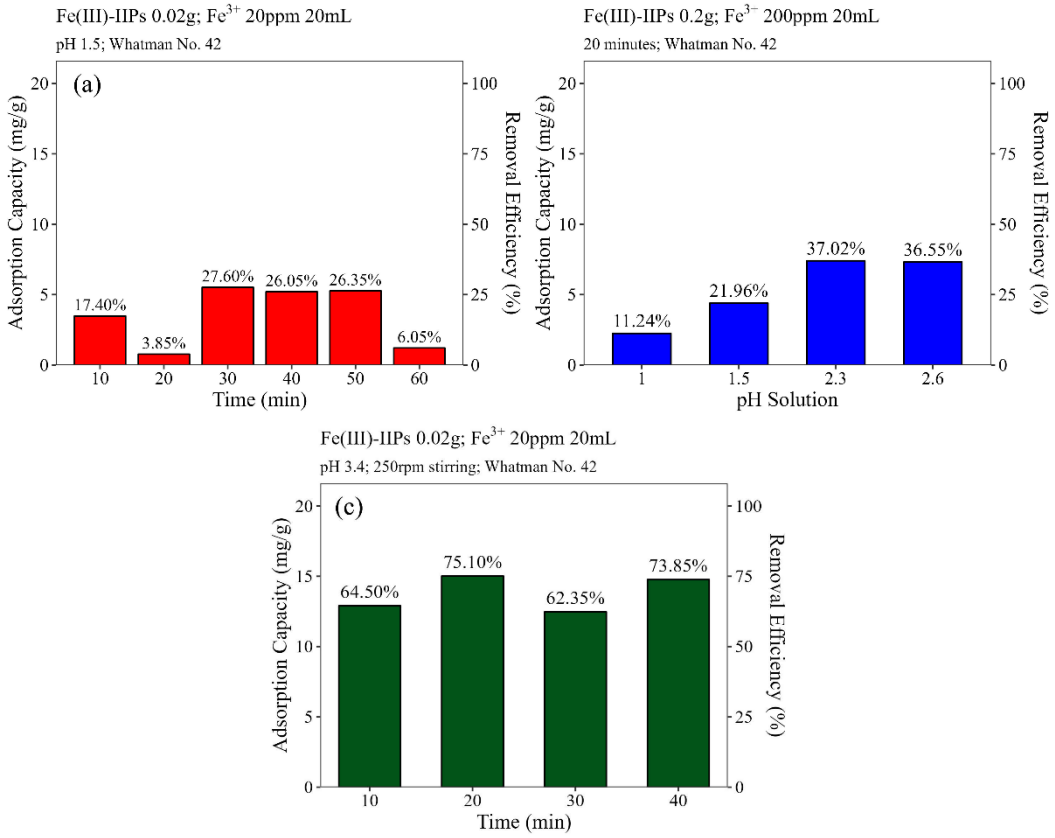

Figure 3. Adsorption System of Fe^{3+} Ion on Fe(III)-IIPs: (a) Condition 1, (b) Condition 2, and (c) Condition 3

Condition 2 shows the adsorption of Fe^{3+} ions at a different pH, i.e., at pH 1, 1.5, 2.3, and 2.6. Apparently there is a tendency for adsorption to increase as the pH increases, with the average adsorption capacity and removal efficiency, respectively, at 5.3 mg/g and 27%. Supporting the analysis of Condition 1, increasing the pH can prevent or reduce protonation of the active site of Fe(III)-IIPs, improving the attraction between adsorbent-adsorbate. However, it should be noticed that the adsorption of condition 2 was performed at higher doses of adsorbent and adsorbate concentrations, 200 mg Fe(III)-IIPs and 200 ppm Fe^{3+}. In total, IIPs-Fe(III) adsorbed more Fe^{3+} ions, which is ±80 ppm (1.5 mg Fe^{3+}), resulting in slightly better performance than the previous system, yet considered lavish in resource. This is possible owing to the limited occupation of Fe(III)-IIPs during the adsorption process, which the adsorbent tends to sink, thus unable to reach adsorbates.

Condition 3 tries to overcome the limited occupation of Fe(III)-IIPs by applying magnetic stirring at 250 rpm during the adsorption and performed at higher pH to produce efficient adsorption of Fe^{3+} ions. Oumani et al. [11] observed that the efficiency of Cr^{3+} ion adsorption tends to increase with increased stirring speed during the process. In addition, the type of stirring can also play an important role, as demonstrated by Kuśmierek and Świątkowski [35] in the adsorption system performed against 4-chlorophenol on the active carbon material. Physically contact stirring (magnetic bar and mechanical overhead) on the adsorbent increases the adsorption capacity, as the contact between the adsorbent and the mixer bar is likely to break down the particles into smaller particles and increase the occupation of adsorbents compared to shaker stirring. However, the adsorption results obtained tend to be irregular and did not increase over time, with the average adsorption capacity and removal efficiency at 13.8 mg/g and 69%, respectively.

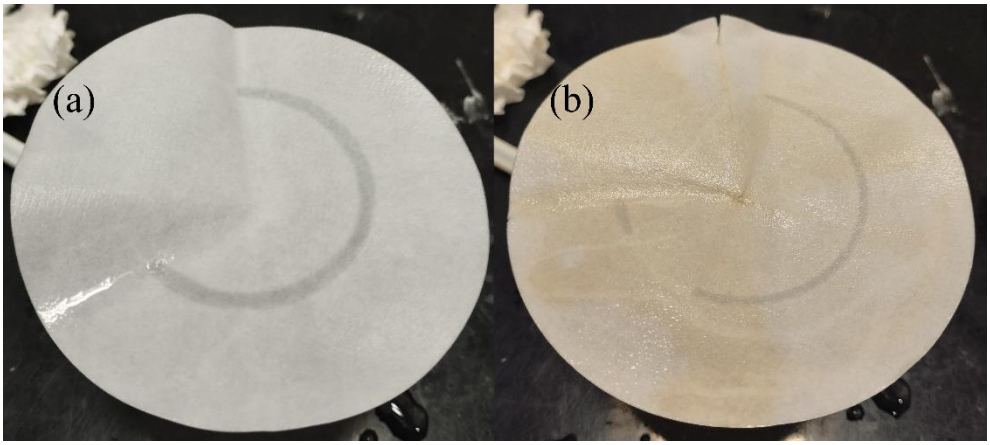

Figure 4. Whatman Filter Paper no. 42: (a) before and (b) after filtration

It can be suspected that the Fe^{3+} ions were being filtered during the filtration process. As described in point 3.1, at higher pH, iron is slowly hydrolyzed to form a species of iron hydroxide that displays a yellowish-brown color. Therefore, it is important to know the optimum pH of the Fe^{3+} ion adsorption, which some studies have shown to be around pH 4 [26],[36]. Figure 4 shows the filter papers were different in color before and after filtration, which can be suspected as iron hydroxide has been filtered on the paper. Merck, as the manufacturer of Whatman 42, classified it as slow filter paper with a porous size of 2.5 µm composed of cellulose polymer [37]. Test on filtration time to filter 20 mL of water at room temperature, measured for 388 seconds at flow rate of 50 µL/s.

This gives a significant error to the adsorption system, especially since cellulose contains many hydroxyl groups (–OH) with the potential for high reactivity and the ability to bind metal ions [38]. Engin et al. [39] explained the adsorptive characteristics of filter paper against several heavy metals, including Fe^{3+} ions. This finding tends to have an impact on low metal concentrations (<50 ppm), but it is still concluded that filter paper should not be involved during the separation of heavy metals in the adsorption process. However, utilizing filter paper is still considered affordable, followed by low consumption of energy; thus, the contact time of adsorbate on the filter paper needs to be shortened, alternatively. Therefore, the increase in adsorption performance on condition 3 was probably caused by errors during filtration.

Table 1. Whatman filter paper performance

Filter paper	Pore size (µm)	Flow rate (µL/s)	Contact time (s)*
Whatman 42	2,5	50	388
Whatman 41	20	360	55

* filtration of 20 mL water

Condition 4 shows as depicted in Figure 5 the adsorption of Fe^{3+} ions at pH 4 and stirring at 250 rpm for varying adsorption times at 5, 15, 30, 45, and 60 minutes. The choice of pH 4 in the system is based on the optimum pH for adsorption of Fe^{3+} ions by the same material in several references [26],[36],[40]. To shorten the contact time of adsorbate on paper, Whatman 41 has been chosen, as it is classified as fast filter paper with pore size of 20 µm [41] and flow rate of 360 µL/s, with a contact time under a minute, as shown in Table 1.

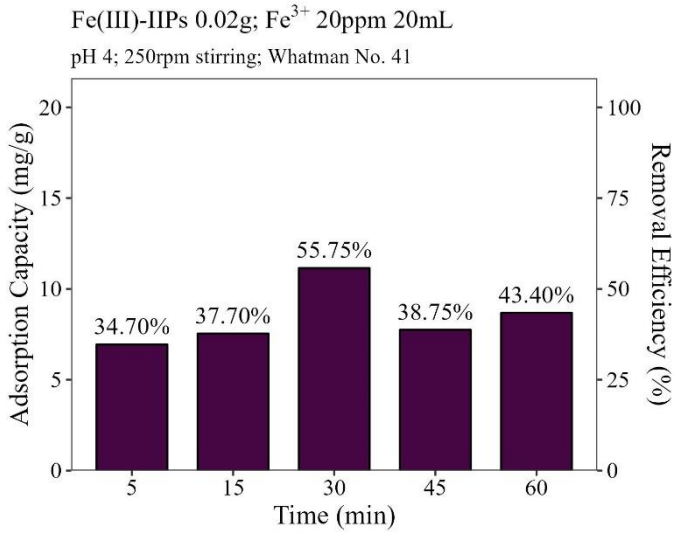

Figure 5. Condition 4 after optimization

There is an increase to a maximum of 55% removal efficiency and adsorption capacity of 11 mg/g at 30 minutes, with the average adsorption capacity and percent absorption during adsorption at 8.4 mg/g and 42%, respectively. However, after that, there is a decline in the 45th minute and a slight increase again in the 60th minute. This may be attributed to the desorption of Fe^{3+} ions after reaching equilibrium at 30 minutes, which is caused by the formation of iron hydroxide species followed by an increase in the concentration of H^+ ions according to Equation 4; thus, there is a tendency for the adsorption system to become more acidic over time.

Based on the modeling carried out on the adsorption kinetics equation, namely pseudo first order (PFO) and pseudo second order (PSO), shown in Figure 6, the standard error of estimate (SEE) parameter shows a smaller number in the PSO equation modeling, which is 2.07 compared to the PFO equation of 2.83. This indicates that the Fe^{3+} adsorption mechanism on Fe(III) IIPs predominantly occurs by chemisorption rather than physisorption [42],[43]. This is

also supported by the statistical parameters AIC and BIC, which have smaller values in PSO compared to PFO. More details are shown in Table 2.

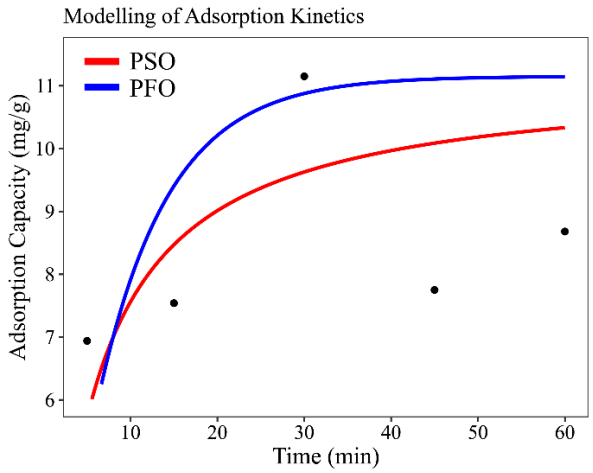

Figure 6. Kinetics Modelling of Fe^{3+} Adsorption on Fe(III)-IIPs

Adsorption kinetics explains the adsorbate transfer process during adsorption and the factors that influence adsorption over time [8], and this can be modeled into two general equations often used, namely PFO and PSO, to achieve an interpretation of the adsorption mechanism that occurs. The chemisorption mechanism dominates adsorption by Fe(III) IIPs, which can be explained by the process of forming active sites on the surface of the adsorbent. The active site formed will selectively recognize the target metal due to its similar chemical properties. So the ability of IIPs to recognize targets is often referred to "lock and key" mechanism [44].

Table 2. Statistics Parameters of Adsorption Modelling

Adsorption Kinetics	Parameters	Value
Pseudo First Order	k (min^{-1})	0.123
	qe (mg/g)	11.15
	SEEs	2.83
	AIC	26.05
	BIC	25.28
Pseudo Second Order	k (min^{-1})	19
	qe (mg/g)	11.15
	SEE	2.07
	AIC	22.91
	BIC	22.13

CONCLUSION

This research seeks to evaluate the Fe^{3+} adsorption system on selective materials, Fe(III)-IIPs. Analysis does not only focus on the results of adsorption but also on in-depth observations regarding the characteristics of Fe^{3+} ions in water, which have a big impact on the development of the adsorption system on various materials. There is a fundamental dilemma and difficulty in the adsorption of Fe^{3+} ions, owing to their elevated solubility in acidic conditions, but this condition prevents ideal adsorption from occurring due to protonation of the adsorbent surface by H^+ ions. Meanwhile, hydrolysis occurs immediately, followed by the precipitation of iron hydroxide at a pH that tends to be in the acidic realm (pH 4.5), thus also inhibiting ideal Fe^{3+}

adsorption. Optimization of pH during adsorption was measured at pH 4, which is very close to the pH when hydroxide formation occurs. Findings during the evaluation of the adsorption system showed that adsorption of Fe^{3+} on Fe(III)-IIPs occurred by chemisorption, which enabled the formation of chemical bonds between Fe^{3+} and active sites on the surface of Fe(III)-IIPs, followed by the maximum adsorption capacity observed reaching 11 mg/g.

ACKNOWLEDGMENTS

The author would like to thank the Institute for Research and Community Service (LPPM) of Sriwijaya University for research funding assistance through *Unggulan Kompetitif* grants with Rector's Decree No. 0013/UN9/SK.LP2M.PT/2024, dated May 20th, 2024.

REFERENCES

1 Aktar, J. 2021. Batch adsorption process in water treatment. In *Intelligent Environmental Data Monitoring for Pollution Management* (pp. 1–24). Elsevier.

2 Edianta, J., Satya, O. C., Virgo, F., Saleh, K., & Royani, I. 2023. Design of potentiometric instrumentation system based on Arduino nano microcontroller using imprinted polymer for the determination of Fe (III) metal ions. *AIP Conference Proceedings*, *2689(1)*, 1–7.

3 Kupai, J., Razali, M., Buyuktiryaki, S., Kecili, R., & Szekely, G. 2017. Long-term Stability and Reusability of Molecularly Imprinted Polymers. *Polymer Chemistry*, *8*(4), 666–673.

4 Bonilla-Petriciolet, A., Mendoza-Castillo, D. I., Piccin, J. S., Cadaval Jr., T. R. S., Pinto, L. A. A. de, Dotto, G. L., Salau, N. P. G., Dura´n-Valle, C. J., Botet-Jimenez, A. B., Omenat-Moran, D., Xu, M., McKay, G., Rivera-Utrilla, J., Sanchez-Polo, M., Ocampo-Perez, R., Altimari, P., Caprio, F. D., Pagnanelli, F., Pouran, S. R., … Bayrami, A. 2017. *Adsorption Processes for Water Treatment and Purification* (H. E. Reynel-Ávila, Ed.; 1st ed.). Springer International Publishing.

5 Musah, M., Azeh, Y., Mathew, J., Umar, M., Abdulhamid, Z., & Muhammad, A. 2022. Adsorption Kinetics and Isotherm Models: A Review. *Caliphate Journal of Science and Technology*, *4*(1), 20–26.

6 Raji, Z., Karim, A., Karam, A., & Khalloufi, S. 2023. Adsorption of Heavy Metals: Mechanisms, Kinetics, and Applications of Various Adsorbents in Wastewater Remediation—A Review. *Waste*, *1*(3), 775–805.

7 Tran, H. D., & Nguyen, D. Q. 2023. Study on methylene blue adsorption using cashew nut shell-based activated carbon. *Chimica Techno Acta*, *10*(4), 1–8.

8 Royani, I., Maimunah, M., Edianta, J., Alfikro, I., Monado, F., Jorena, J., Satya, O. C., & Virgo, F. 2024. Synthesis of Ion Imprinted Polymers (IIPs) Adsorbent Materials Using Fe(III) Leaching Process with Variation of Hydrochloric Acid Solvent Concentration and Heat Treatment. *Science and Technology Indonesia*, *9*(2), 336–344.

9 Yang, P., Cao, H., Mai, D., Ye, T., Wu, X., Yuan, M., Yu, J., & Xu, F. 2020. A novel morphological ion imprinted polymers for selective solid phase extraction of Cd(II): Preparation, adsorption properties and binding mechanism to Cd(II). *Reactive and Functional Polymers*, *151*, 104569.

10 Cruz-Lopes, L. P., Macena, M., Esteves, B., & Guiné, R. P. F. 2021. Ideal pH for the adsorption of metal ions Cr^{6+}, Ni^{2+}, Pb^{2+} in aqueous solution with different adsorbent materials. *Open Agriculture*, *6*(1), 115–123.

11 Oumani, A., Mandi, L., Berrekhis, F., & Ouazzani, N. 2019. Removal of Cr^{3+} from tanning effluents by adsorption onto phosphate mine waste: Key parameters and mechanisms. *Journal of Hazardous Materials*, *378*, 120718.

12 Shi, M., Min, X., Ke, Y., Lin, Z., Yang, Z., Wang, S., Peng, N., Yan, X., Luo, S., Wu, J., & Wei, Y. 2021. Recent progress in understanding the mechanism of heavy metals retention by iron (oxyhydr)oxides. *Science of The Total Environment*, *752*(141930), 1–19.

13 Darmawan, W., Nurani, D. A., Rahayu, D. U. C., & Abdullah, I. 2020. Synthesis of ion imprinted polymer for separation and preconcentration of iron(III). *AIP Conference Proceedings*, *2242(1)*, 040025.

14 Weller, M., Overton, T., Rourke, J., & Armstrong, F. 2014. *Inorganic Chemistry* (Sixth edition). Oxford University Press.
15 Khatri, N., Tyagi, S., & Rawtani, D. 2017. Recent strategies for the removal of iron from water: A review. *Journal of Water Process Engineering*, *19*(5), 291–304.
16 Gulcin, İ., & Alwasel, S. H. 2022. Metal Ions, Metal Chelators and Metal Chelating Assay as Antioxidant Method. *Processes*, *10*(1), 132.
17 Adams, P. C. 2015. Epidemiology and diagnostic testing for hemochromatosis and iron overload. *International Journal of Laboratory Hematology*, *37*(S1), 25–30.
18 Giove, A., El Ouardi, Y., Sala, A., Ibrahim, F., Hietala, S., Sievänen, E., Branger, C., & Laatikainen, K. 2023. Highly selective recovery of Ni(II) in neutral and acidic media using a novel Ni(II)-ion imprinted polymer. *Journal of Hazardous Materials*, *444*(130453), 1–10.
19 Novianty, N., Edianta, J., Jorena, J., Saleh, K., Bama, A. A., Koriyanti, E., Ariani, M., & Royani, I. 2023. Synthesis of Fe(III)-IIPs (Ion Imprinted Polymers): Comparing Different Concentrations of HCl and HNO_3 Solutions in the Fe(III) Polymer Extraction Process for Obtaining the Largest Cavities in Fe(III)-IIPs. *Science and Technology Indonesia*, *8*(3), 361–366.
20 Flynn, C., M. 1984. Hydrolysis of Inorganic Iron(III) Salts. *Chemical Reviews*, *84*, 31–41.
21 Scholz, M. 2006. *Wetland systems to control urban runoff* (1. ed). Elsevier.
22 Brown, T. L., LeMay, Jr., H. E., Bursten, B. E., Murphy, C. J., & Woodward, P. M. 2012. *Chemistry: The Central Science* (12th ed). Prentice Hall.
23 Weber, B. 2023. *Coordination Chemistry: Basics and Current Trends*. Springer Berlin Heidelberg.
24 Sutherland, T. I., Sparks, C. J., Joseph, J. M., Wang, Z., Whitaker, G., Sham, T. K., & Wren, J. C. 2017. Effect of ferrous ion concentration on the kinetics of radiation-induced iron-oxide nanoparticle formation and growth. *Physical Chemistry Chemical Physics*, *19*(1), 695–708.
25 Darweesh, M. A., Elgendy, M. Y., Ayad, M. I., Ahmed, A. M., Elsayed, N. M. K., & Hammad, W. A. 2022. Adsorption isotherm, kinetic, and optimization studies for copper(II) removal from aqueous solutions by banana leaves and derived activated carbon. *South African Journal of Chemical Engineering*, *40*, 10–20.
26 Roushani, M., Beygi, T. M., & Saedi, Z. 2016. Synthesis and application of ion-imprinted polymer for extraction and pre-concentration of iron ions in environmental water and food samples. *Spectrochimica Acta Part A: Molecular and Biomolecular Spectroscopy*, *153*(1), 637–644.
27 Gore, P. M., Khurana, L., Siddique, S., Panicker, A., & Kandasubramanian, B. 2018. Ion-imprinted electrospun nanofibers of chitosan/1-butyl-3-methylimidazolium tetrafluoroborate for the dynamic expulsion of thorium(IV) ions from mimicked effluents. *Environmental Science and Pollution Research*, *25*(4), 3320–3334.
28 Kim, J., Kang, T., Kim, H., Shin, H. J., & Oh, S.-G. 2019. Preparation of PVA/PAA nanofibers containing thiol-modified silica particles by electrospinning as an eco-friendly Cu (II) adsorbent. *Journal of Industrial and Engineering Chemistry*, *77*, 273–279.
29 Rajhans, A., Gore, P. M., Siddique, S. K., & Kandasubramanian, B. 2019. Ion-imprinted nanofibers of PVDF/1-butyl-3-methylimidazolium tetrafluoroborate for dynamic recovery of Europium(III) ions from mimicked effluent. *Journal of Environmental Chemical Engineering*, *7*(3), 1–12.
30 Wirawan, T., Supriyanto, G., & Soegianto, A. 2019. Preparation of a New Cd(II)-Imprinted Polymer and Its Application to Preconcentration and Determination of Cd(II) Ion from Aqueous Solution by SPE-FAAS. *Indonesian Journal of Chemistry*, *19*(1), 97.
31 Chi, Z., Zhu, Y., Liu, W., Huang, H., & Li, H. 2021. Selective removal of As(III) using magnetic graphene oxide ion-imprinted polymer in porous media: Potential effect of external magnetic field. *Journal of Environmental Chemical Engineering*, *9*(4), 1–10.
32 Luu, T.-T., Dinh, V.-P., Nguyen, Q.-H., Tran, N.-Q., Nguyen, D.-K., Ho, T.-H., Nguyen, V.-D., Tran, D. X., & Kiet, H. A. T. 2022. Pb(II) adsorption mechanism and capability from aqueous solution using red mud modified by chitosan. *Chemosphere*, *287*(132279), 1–8.

33 Indah, S., Helard, D., & Binuwara, A. 2018. Studies on desorption and regeneration of natural pumice for iron removal from aqueous solution. *Water Science and Technology*, *2017*(2), 509–515.
34 Mishra, S. P. 2014. Adsorption–desorption of heavy metal ions. *Current Science*, *107*(4), 601–612.
35 Kuśmierek, K., & Świątkowski, A. 2015. The influence of different agitation techniques on the adsorption kinetics of 4-chlorophenol on granular activated carbon. *Reaction Kinetics, Mechanisms and Catalysis*, *116*(1), 261–271.
36 Gomaa, H., Sayed, A., Mahross, M. H., Abdel-Hakim, M., Othman, I. M. M., Li, J., & El-Bahy, S. M. 2022. A hybrid spongy-like porous carbon-based on azopyrazole-benzenesulfonamide derivative for highly selective Fe^{3+}-adsorption from real water samples. *Microporous and Mesoporous Materials*, *330*, 1–13.
37 Merck KGaA, M. 2024. *Whatman® quantitative filter paper, ashless, Grade 42* [Specification]. Whatman® Quantitative Filter Paper, Ashless, Grade 42. Online: https://www.sigmaaldrich.com/ID/en/product/aldrich/wha1442110#product-documentation.
38 Daochalermwong, A., Chanka, N., Songsrirote, K., Dittanet, P., Niamnuy, C., & Seubsai, A. 2020. Removal of Heavy Metal Ions Using Modified Celluloses Prepared from Pineapple Leaf Fiber. *ACS Omega*, *5*(10), 5285–5296.
39 Engin, M. S., Uyanik, A., Cay, S., & Icbudak, H. 2010. Effect of the Adsorptive Character of Filter Papers on the Concentrations Determined in Studies Involving Heavy Metal Ions. *Adsorption Science & Technology*, *28*(10), 837–846.
40 Saatçılar, Ö., Şatıroğlu, N., Say, R., Bektaş, S., & Denizli, A. 2006. Binding behavior of Fe^{3+} ions on ion-imprinted polymeric beads for analytical applications. *Journal of Applied Polymer Science*, *101*(5), 3520–3528.
41 Merck KGaA, M. 2024. *Whatman® quantitative filter paper, ashless, Grade 41* [Specification]. Whatman® Quantitative Filter Paper, Ashless, Grade 41. https://www.sigmaaldrich.com/ID/en/product/aldrich/wha1441125.
42 He, W., Yu, Q., Wang, N., & Ouyang, X. 2020. Efficient adsorption of Cu(II) from aqueous solutions by acid-resistant and recyclable ethylenediamine tetraacetic acid-grafted polyvinyl alcohol/chitosan beads. *Journal of Molecular Liquids*, *316*, 113856.
43 Praipipat, P., Ngamsurach, P., & Sanghuayprai, A. 2023. Modification of sugarcane bagasse with iron(III) oxide-hydroxide to improve its adsorption property for removing lead(II) ions. *Scientific Reports*, *13*(1), 1467.
44 Hande, P. E., Samui, A. B., & Kulkarni, P. S. 2015. Highly selective monitoring of metals by using ion-imprinted polymers. *Environmental Science and Pollution Research*, *22*(10), 7375–74